



## DEVELOPMENT AND CHARACTERIZATION OF NEW BIOCOMPATIBLE POLYESTER HERNIA MESHES IMPREGNATED WITH CHITOSAN

GRADISTEANU PIRCALABIORU Gratiela<sup>1,2</sup>, DOLETE Georgiana<sup>1</sup>,  
TIHAUAN Bianca<sup>1</sup>, VISILEANU Emilia<sup>3</sup>, AXINIE (BUCOS) Madalina<sup>1</sup>

<sup>1</sup> Research and Development Department of SC Sanimed International Impex SR, Sos. București Măgurele 70F,  
Bucharest 051434, Romania, E-Mail: [gratiela.pircalabioru@bio.unibuc.ro](mailto:gratiela.pircalabioru@bio.unibuc.ro)

<sup>2</sup> Research Institute of University of Bucharest (ICUB), University of Bucharest, 91-95 Splaiul Independentei,  
Bucharest, 050095, Bucharest, Romania

<sup>3</sup> The National Research and Development Institute for Textiles and Leather, 16 Lucretiu Patrascanu, Bucharest Romania,  
E-Mail: [visilean@certex.ro](mailto:visilean@certex.ro)

Corresponding author: Visileanu Emilia, E-mail: [e.visileanu@incdtp.ro](mailto:e.visileanu@incdtp.ro)

**Abstract:** *Hernias and abdominal wall defects are routinely treated using synthetic and biological meshes. However, complications such as hernia recurrence and seroma and adhesion formation are quite common. So far, various materials have been employed to prevent adhesions while ensuring good mechanical properties. A good hernia mesh should harbor outstanding parietal surface tissue in-growth with minimal visceral surface adhesiveness. A good way to minimize the disadvantages of surgical meshes is to combine synthetic and natural polymers to ensure adequate biomechanical properties, or to design innovative meshes that can replace current hernia meshes. In this study, we have designed polyester (PES) meshes impregnated with chitosan that exhibited increased biocompatibility. These preliminary results pave the way for future ex vivo and in vivo studies.*

**Key words:** *hernia mesh, chitosan, polyester, abdominal hernia repair, novel textiles*

### 1. INTRODUCTION

The restoration of defects from surgical incisions requires the use of prosthetic implants, which can cause various long-term complications, such as: rejection/infection of the graft used, fistula formation or hernia relapse [1, 2]. Surgical meshes made of synthetic polymers are the 'gold standard', being used for all types of hernia [3]. The use of these polymer meshes demonstrated a significant reduction in the rate of relapse, pain minimisation, overall improving overall post-operative results. Although a wide range of surgical meshes have been designed and used in hernia healing procedures, no mesh has yet demonstrated a sufficiently strong structure to simultaneously promote the remodeling of the host tissue. In general, non-resorbable synthetic meshes made of polypropylene, polyesters and expanded polytetrafluorethylene are generally used, and resorbable meshes are made of polyglycolic acid and carboxycellulose. In parallel, several models of biological surgical nets derived from bovine pericardium and pig or human acellularized dermis have been



designed [1-6]. Their use is not very well known given the complications arising from the use of xenografts and the extremely high cost of production.

A good way to combat the disadvantages of surgical meshes is to combine synthetic polymers with natural ones to ensure adequate biomechanical properties, or to design innovative hernia meshes that can replace currently available meshes.

An example of material used successfully in the biomedical field is chitosan, derived from chitin, the most widespread natural polymer after cellulose, which is found in the exoskeleton of arthropods or in the cell walls of fungi and yeast. Chitosan is obtained by partial deacetylation of chitin (minimum 50%). The obtained chitosan is a natural, biocompatible, biodegradable polymer, has the property to form films, has a high mechanical strength and is easy to chemically modify [7-9]. In recent years there has been an increased interest in the use of chitosan and chitin, with studies focusing both on the controlled release properties of active substances and on their ability to help regeneration tissues with applications covering a large range in tissue and regenerative engineering.

## 2. MATERIALS AND METHODS

### 2.1 Impregnation of polyester and polyamide fabrics with chitosan

The polyester fabrics (with different pore sizes: P1-0.9 mm, P2-1.66mm, P3-1.08mm, P4-1.2mm) were cut into 1x1 cm<sup>2</sup> pieces and hydrolysed in a basic solution in order to modify their surface. The textiles alkalinized in a solution of 12% sodium hydroxide for 90 minutes at 60°C. They were then rinsed with distilled water and acetone to remove any traces of impurities. The materials were then dried in the oven at 80°C for 10 minutes, and the fiber surface is subsequently modified by immersing the textile materials in 2% chitosan solution, previously dissolved in a 2M acetic acid solution. The immersion stage is followed by a drying at 60°C for one hour, rinsing with distilled water of the samples and a final drying at 70°C for 10 minutes. When alkalinized polyester fibers are treated with cationic agents, the hydroxyl and carboxyl groups, available on the fiber surface, will participate in the formation of hydrogen or electrostatic bonds with the functional groups of the cationic agent.

The characterization of the obtained material was performed by Fourier transform (FT-IR) infrared spectroscopy. The FT-IR spectra analysis was used to confirm the impregnation of the synthetic fabrics with chitosan. In parallel, a control test was used in order to check if the impregnation steps (alkalinization, drying, washing with distilled water and acetone) can affect the structure of the materials.

The materials were analysed before and after the alkalinization of the surfaces to determine whether the fibers undergo changes following hydrolysis treatment in the basic environment. Finally, the fibres coated with chitosan were analyzed to confirm the coating of the fibres with chitosan by the impregnation method. The synthesized materials were characterized after their drying by Fourier transformed infrared spectroscopy using a Nicolet iS50FT-IR spectrophotometer (Thermo Scientific, Massachusetts, USA), equipped with a DTGS detector. The spectra were measured in the spectral range 4000-400 cm<sup>-1</sup>, with a resolution of 4 cm<sup>-1</sup> and 32 scans.

### 2.2. Biocompatibility assessment

Biocompatibility was analysed using the MTT and LDH tests a previously described [10]. MTT assay is a quantitative test which allows evaluation of both cell viability and proliferation. Briefly, HCT-8 epithelial cells were incubated with 1 mg/ml [3-(4,5-dimethylthiazol-2-yl)]-2,5-diphenyltetrazolium bromide (MTT) solution for 4 h in the dark, at 37°C. Formazan crystals were solubilized with HCl-SDS, resulting in purple solution, quantified by spectrophotometry at 570 nm, using FlexStation3 (Molecular Devices, USA).

The LDH test (Tox7 kit, Sigma-Aldrich) was performed according to manufacturer's instructions. Cells that no longer have membrane integrity release lactate dehydrogenase (LDH) into the culture medium. The culture medium was collected and mixed with the kit's components in order to be evaluated 4 days of culture by spectrophotometric readings at 490 nm.

For qualitative analysis of biocompatibility, cells were stained with fluorescein diacetate (FDA) and cell morphology was analysed by microscopy (Carl Zeiss AxioScope, Jena, Germany) and then processed with Zeiss Zen 2010 software. Statistical analysis was performed using Graph Pad Prism 6.0 software, Unpaired t-test. Statistically significant values were considered for  $p < 0.05$ .

### 3. RESULTS

The FTIR spectra in Figure 1 (left panel) is characteristic of chitosan, being defined by the presence of absorption bands at  $3361$  and  $3291$   $\text{cm}^{-1}$ , specific to the vibrations of the stretching of the O-H and N-H bonds, as well as the hydrogen bonds in the structure of the chitosan. The two signals at  $2921$  and  $2877$   $\text{cm}^{-1}$  are generally specific to polysaccharides, which can be attributed to the asymmetric and symmetrical valence vibrations of the  $\text{sp}^3\text{C-H}$  bonds. The presence of *n*-ethylate group residues is confirmed by the absorption bands characteristic of the valence vibrations of the following functional groups:  $1656$   $\text{cm}^{-1}$  for  $\nu(\text{C=O})$  of the primary amides, at  $1550$   $\text{cm}^{-1}$  for  $\nu(\text{N-H})$  of the secondary amides, respectively at  $1254$   $\text{cm}^{-1}$  for  $\nu(\text{C-N})$  of tertiary amides. The presence of methylene and methyl groups is confirmed by the signals from  $1415$  and  $1375$   $\text{cm}^{-1}$  attributed to the deformation vibrations of  $\text{CH}_2$  and the symmetrical vibrations of the  $\text{CH}_3$ . The absorption band from  $1153$   $\text{cm}^{-1}$  can be attributed to asymmetric vibration movements in the etheral decks C-O-C, and those at  $1060$  and  $1018$   $\text{cm}^{-1}$  correspond to the valence vibrations of the functional C-O grouping. The not very intense signal from  $1260$   $\text{cm}^{-1}$  is attributed to the hydroxyl groups present in the chitosan, and finally the absorption band from  $1896$   $\text{cm}^{-1}$  is characteristic of the deformation vibrations outside the plane of the C-H bonds in the pyranosic cycle of the monosaccharides.

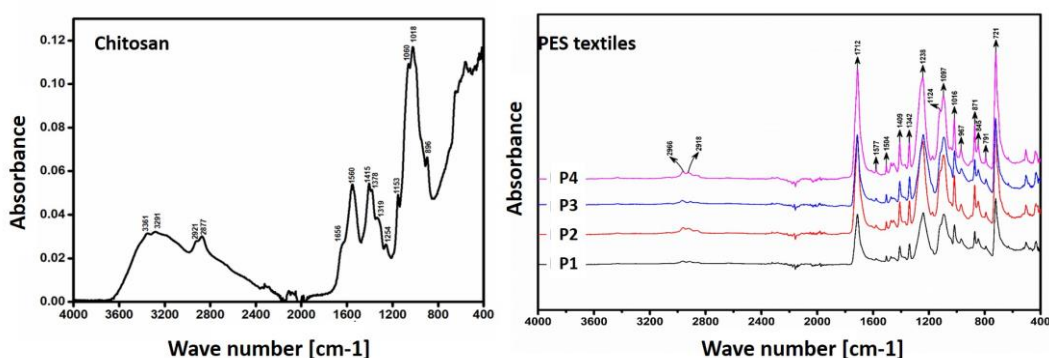


Fig. 1: FT-IR spectra for chitosan and PES textiles (PES meshes with different pore sizes)

The characteristic absorption of the spectra of untreated materials (Figure 1, right panel) is based in principle on the absorption band located at  $1712$   $\text{cm}^{-1}$ , characteristic of the valence vibrations of the carbonyl bonds  $\text{C=O}$ , the absorption bands specific to the asymmetrical and symmetrical elongation of the  $\text{sp}^3\text{C-H}$  bonds at  $2966$  and  $2918$   $\text{cm}^{-1}$ , but also the presence of absorption bands of low intensity, in the range  $1600$ - $1500$   $\text{cm}^{-1}$ , characteristic of the valence vibrations of  $\text{C=C}$  of aromatic compounds. In addition, the fingerprint areas of the region  $1400$ - $400$   $\text{cm}^{-1}$  confirm typical polyester structures, namely the terephthalate polyethylene:  $1409$  and  $1342$   $\text{cm}^{-1}$  are specific to the ethylene glycol segment, while  $1238$  and  $1124$   $\text{cm}^{-1}$  are specific to the grouping

terephthalate (-OOC-C-H-COO), and the vibrations of the methylene group related to C-O can be identified at 1097 cm<sup>-1</sup>. The spectra obtained for the four samples (P1-P4) are similar to other spectra in PET-specific literature.

IR spectra of alkaline-activated materials was similar to the untreated ones. They mainly show a attenuation of intensities, a slight change in the strips' gorges or a displacement of the maximum absorption compared to the typical bands of untreated materials (Figure 2).

The impregnation of chitosan on the surfaces of the two types of fibres was successfully carried out according to the spectra obtained from their impregnation. The spectra obtained on the 4 polyester fibre samples (Figure 3(a-d)) can confirm their coating with chitosan by forming the absorption band at approximately 3400 cm<sup>-1</sup>, which can be attributed to both the existence of the N-H groups in the molecular formula of the chitosan, as well as the formation of hydrogen bonds between polyesters and chitosan. In contrast, in the case of the polyamide sample Figure 13(e), the two spectra are identical. Firstly, it can be confirmed that both polyester fibres and polyamid fibres have not undergone changes following treatment with NaOH 12% solution at 60 °C. After immersion in 2% chitosan solution, polyester fibres demonstrated a good ability to interact with chitosan by forming hydrogen bonds.

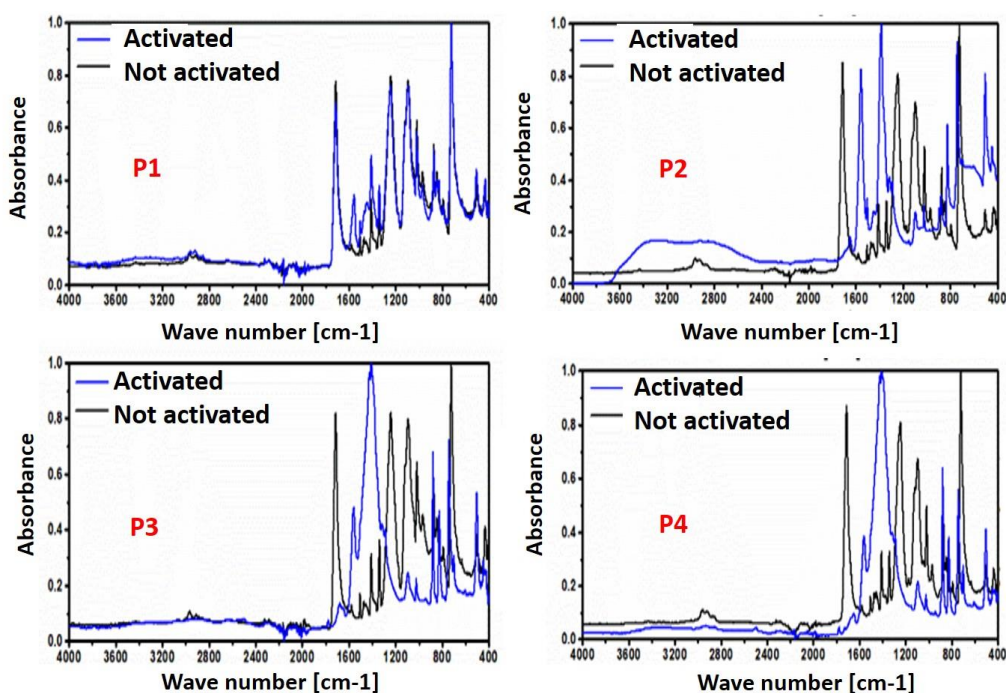


Fig. 2: FT-IR spectra for activated samples using alkaline treatment

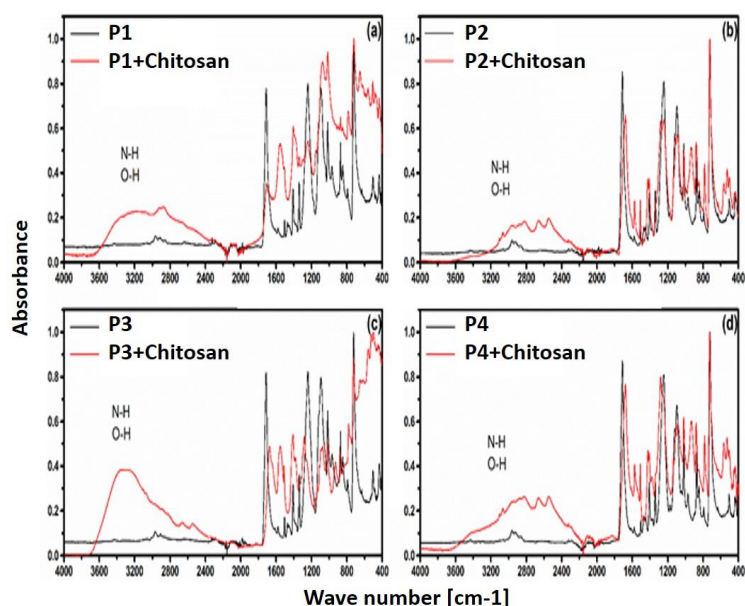


Fig. 3: FT-IR spectra for the textiles impregnated with chitosan

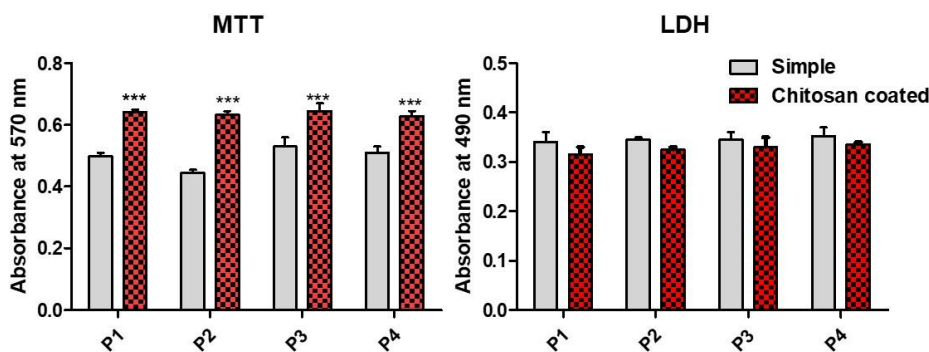


Fig. 4: Effect of chitosan coating on the mesh biocompatibility,  $n=2$

The biocompatibility analysis was done using MTT and LDH test. While MTT measures cells proliferation, the LDH test quantifies cytotoxicity. We have observed that chitosan treatment significantly enhanced cell proliferation for all tested samples whereas the cytotoxicity remained unmodified.

#### 4. CONCLUSIONS

Abdominal hernia repair is generally done using surgical meshes made up of various biomaterials. However, no ideal hernia mesh exists and current research efforts are focused on developing meshes with different fiber size and porosity by using a variety of manufacturing methods and implantation procedures. Importantly, surface modification methods are potent areas of opportunity to retain material strength and increase biocompatibility of available meshes. We describe here the development of new PES meshes coated with chitosan aimed for better hernia



repair management. These meshes exhibited good biocompatibility *in vitro* but further *in vivo* studies are required.

**Acknowledgements.** The authors gratefully acknowledge the financial support of the ManuNet grant PariTex (grant no. 95/2019).

## REFERENCES

- [1] U. Klinge, B. Klosterhalfen; *Modified classification of surgical meshes for hernia repair based on the analyses of 1,000 explanted meshes*; *Hernia* (2012) 16:251–258, DOI 10.1007/s1002901209136.
- [2] Baylón K, Rodríguez-Camarillo P, Elías-Zúñiga A, Díaz-Elizondo JA, Gilkerson R, Lozano K. Past, Present and Future of Surgical Meshes: A Review. *Membranes (Basel)*. 2017;7(3):47. Published 2017 Aug 22. doi:10.3390/membranes7030047
- [3] Bendavid R., Abrahamson J., Arregui M.E., Flament J.B., Phillips E.H. *Abdominal Wall Hernias: Principles and Management*. 1st ed. Springer; New York, NY, USA: 2001.
- [4] Pandit A.S., Henry J.A. Design of surgical meshes—An engineering perspective. *Technol. Heal. Care*. 2004;12:51–65.
- [5] Schumpelick V., Fitzgibbons R.J. *Hernia Repair Sequelae*. 1st ed. Springer; Berlin/Heidelberg, Germany: 2010.
- [6] Cortes R.A., Miranda E., Lee H., Gertner M.E. Biomaterials and the evolution of hernia repair II: Composite meshes. In: Norton J., Barie P.S., Bollinger R.R., Chang A.E., Lowry S., Mulvihill S.J., Pass H.I., Thompson R.W., editors. *Surgery*. 2nd ed. Volume 11. Springer; New York, NY, USA: 2008. pp. 2305–2315.
- [7] Paulo N.M. De Brito e Silva M.S. Moraes A.M. Rodrigues A.P. De Menezes L.B. Miguel M.P., et al. Use of chitosan membrane associated with polypropylene mesh to prevent peritoneal adhesion in rats. *J Biomed Mater Res Part B Appl Biomater*. 2009; 91:221
- [8] Kim I.-Y. Seo S.-J. Moon H.-S. Yoo M.-K. Park I.-Y. Kim B.-C., et al. Chitosan and its derivatives for tissue engineering applications. *Biotechnol Adv*. 2008; 26: 1
- [9] VandeVord P. Matthew H. DeSilva S. Mayton L. Wu B. Wooley P. Evaluation of the biocompatibility of a chitosan scaffold in mice. *J Biomed Mater Res*. 2002; 59:585
- [10] Axinie (Bucos) M, Tihauan B, Ivanof A, Pircalabioru GG, Visileanu E, Aydin S, Mihai C, Scarlat R, Vladu A. Development and preliminary characterisation of novel textiles for abdominal hernia repair. *Rom Biotechnol Lett*. 2019; 24(6): 1090-1096. DOI: 10.25083/rbl/24.6/1090.1096